

1 OPTICAL TRAPPING AND ORIENTATION MANIPULATION OF 2D INORGANIC

2 MATERIALS USING A LINEARLY POLARIZED LASER BEAM

3

4 MAKOTO TOMINAGA<sup>1</sup>, YUKI HIGASHI<sup>2</sup>, TAKUYA KUMAMOTO<sup>3</sup>, TAKASHI NAGASHITA<sup>4</sup>,

5 TERUYUKI NAKATO<sup>3</sup>, YASUTAKA SUZUKI<sup>1,2,4</sup> AND JUN KAWAMATA<sup>1,2,4</sup>

6

7 <sup>1</sup>Graduate School of Medicine, Yamaguchi University, 1677-1 Yoshida, Yamaguchi-shi,

8 Yamaguchi 753-8512, Japan

9 <sup>2</sup>Faculty of Science, Department of Biology and Chemistry, Yamaguchi University,

10 1677-1 Yoshida, Yamaguchi-shi, Yamaguchi 753-8512, Japan

11 <sup>3</sup>Department of Applied Chemistry, Kyusyu Institute of Technology, 1-1 Sensui-cho,

12 Tabata-ku, Kitakusyu-shi, Fukuoka 804-8550, Japan

13 <sup>4</sup>Graduate School of Sciences and Technology for Innovation, Yamaguchi University,

14 1677-1 Yoshida, Yamaguchi-shi, Yamaguchi 753-8512, Japan

15

16 Abstract—Owing to the large anisotropy of inorganic nanosheets, such as clay minerals,  
17 the orientation manipulation of nanosheets is an important challenge for realizing future  
18 functional materials. In this study, the methodology for a novel nanosheet manipulation  
19 by using laser radiation pressure is proposed. When a linearly polarized laser beam was  
20 used to irradiate a niobate nanosheet colloid, the nanosheet was trapped at the focal point  
21 so that its in-plane direction was oriented parallel to the propagation direction of the  
22 incident laser beam so as to minimize the scattering force. In addition, the trapped  
23 nanosheet was aligned along the polarization direction of the linearly polarized laser beam.  
24 Thus, a unidirectional alignment of nanosheet can be realized simply by irradiation with  
25 a laser beam.

26 Key Words—Laser Radiation Pressure, Optical Trapping, Polarized Laser Beam, Two-  
27 dimensional Inorganic Material.

## 28 INTRODUCTION

29 Optical manipulation is a technique for non-contact and non-invasive trapping, and  
30 for the transport of colloidal particles by the radiation pressure of a tightly focused laser  
31 beam (Ashkin, 1992; Dholakia *et al.*, 2008). The pressure arises from a momentum  
32 change of a photon when the photon is reflected or refracted by a particle. The size of the  
33 target particles is generally on the scale of sub- $\mu\text{m}$  to several tens of  $\mu\text{m}$ . Typically,

34 spherical shaped particles, such as latex particles (Wright *et al.*, 1994; Won *et al.*, 1999),  
35 glass beads (Ashkin *et al.*, 1986), and metal nanoparticles (Ohlinger *et al.*, 2011;  
36 Lehmuskero *et al.*, 2015), have been manipulated. The target particles are trapped at the  
37 focal point of an incident laser beam, the point at which the strongest trapping field is  
38 produced by the radiation pressure. The trapping is relaxed when the laser irradiation  
39 ceases. The optical manipulation realizes on-demand particle trapping and release by the  
40 on-off switching of the incident laser beam.

41 Recently, optical manipulation has been extended from spherical particles to one-  
42 dimensional (1D) rod-like particles such as carbon nanotubes (Wu *et al.*, 2017),  
43 nanowires (Tong *et al.*, 2010; Yan *et al.*, 2012), and nanofibers (Neves *et al.*, 2010).  
44 Although the 1D particles are trapped at the focal point as well as the spherical particles,  
45 the radiation pressure contributes to the orientation manipulation of the 1D particles.  
46 Namely, the particles are oriented with their long-axis parallel to the propagation direction  
47 of the incident laser beam. The results have establish optical manipulation as an alignment  
48 technique for anisotropic particles.

49 Recent developments of various nanoparticles have evoked interests in two-  
50 dimensional (2D) plate-like particles in addition to 1D particles. In particular, inorganic  
51 nanosheets prepared by exfoliation of layered crystals, such as clay minerals, have

52 attracted great attention owing to their high shape anisotropy (Nakato *et al.*, 2017). A  
53 variety of nanosheets have been prepared and examined as building blocks of functional  
54 nanoassemblies. Oxide nanosheets of smectite-type clay minerals and other layered  
55 oxides have been applied for layer-by-layer assemblies, thin films, porous solids,  
56 inorganic-polymer hybrids, and so forth (Suzuki *et al.*, 2012; Schoonheydt, 2014; Okada  
57 *et al.*, 2015; Tominaga *et al.*, 2016). Because the nanosheets are provided as their colloids  
58 in many cases, manipulation of colloidal nanosheets provides a novel fundamental  
59 technique for assembling the nanosheets.

60 In contrast to spherical and 1D particles, 2D particles are characterized by their biaxial  
61 shape, which requires an orthogonal application of two external forces for uniform, or  
62 unidirectional alignment. This has been realized for colloidal nanosheets of an exfoliated  
63 layered niobium oxide; unidirectional nanosheet alignment was realized under orthogonal  
64 application of an electric field and gravity (Nakato *et al.*, 2014). However, optical  
65 manipulation of 2D plate-like materials has not been attempted to date.

66 In this study, optical manipulation of colloidal nanosheets dispersed in water was  
67 conducted by irradiation with a linearly polarized laser beam. As a model of a nanosheet,  
68 negatively charged niobate ( $\text{Nb}_6\text{O}_{17}^{4-}$ ) was employed because its orientation behavior by  
69 an external field has extensively been studied in recent years (Nakato *et al.*, 2011; Nakato

70 et al., 2014; Nakato et al., 2017). When a laser beam, as an external field, is applied to  
71 colloidal nanosheets, the 2D particles should be trapped at the focal point due to the  
72 strongest trapping field and oriented with one of their axes parallel to the propagation  
73 direction of the incident laser beam as is the case of optical manipulation of 1D particles.  
74 In addition, the other axis of trapped 2D particles should be aligned parallel to the optical  
75 electric field of the linearly polarized laser beam because nanosheets are aligned along to  
76 an alternating electric field due to their high shape anisotropy. As a result, a unidirectional  
77 alignment of a nanosheet is expected to be realized by one external force of a linearly  
78 polarized laser beam.

## 79 EXPERIMENTAL SECTION

### 80 *Sample preparation*

81 A niobate nanosheet colloid, where negatively charged oxide nanosheets are  
82 accompanied by propylammonium ions as their counterions, was prepared by  
83 exfoliation of layered  $K_4Nb_6O_{17}$  according to the previously reported method (Miyamoto  
84 and Nakato, 2004; Nakato *et al.*, 2014). The nanosheet concentration was  $0.05 \text{ g L}^{-1}$  and  
85 the colloid sample exhibited an isotropic phase at room temperature. The lateral lengths  
86 of the nanosheets obtained from transmission electron microscopy (TEM) observations  
87 exhibited a size distribution that obeyed a log-normal distribution to give an average size

88 of 1.6  $\mu\text{m}$ .

89 *Optical microscopy*

90 The colloid sample was injected into a thin-layer glass cell with a 100  $\mu\text{m}$  thickness.

91 The cell was set on the stage of an inverted microscope (IX70, Olympus, Tokyo, Japan).

92 Figure 1 shows a photograph of the experimental setup. A linearly polarized continuous-

93 wave laser beam emitting at 532 nm (Millennia Pro, Spectra Physics, Santa Clara,

94 California, United States) was focused at the center of the cell (50  $\mu\text{m}$  from the cell-

95 sample interface) using an objective lens (Apo, 40 $\times$ , numerical aperture = 0.90, Olympus,

96 Tokyo, Japan) at room temperature. The polarization direction of the linearly polarized

97 laser beam with respect to the sample was varied by rotating a half-wave plate mounted

98 on a stepper motor. The laser power was set at 20 mW after the objective lens. The beam

99 diameter was adjusted to the pupil diameter of the objective lens using a beam expander.

100 The resulting beam waist at the focal point was calculated to be 0.4  $\mu\text{m}$ .

101 For optical microscopy observation upon irradiation with a laser beam, the sample

102 was illuminated by a halogen lamp and the image was monitored with a digital camera

103 (ORCA-Flash 4.0 V3, Hamamatsu Photonics, Hamamatsu, Japan). The incident laser

104 beam was completely blocked by a dichroic mirror and a band pass filter inserted before

105 the camera. Spatial resolutions and the depth of field in the experimental setup were

106 approximately 440 and 420 nm, respectively, which were almost the same sizes as the  
107 diffraction limits. The depth of field was 0.42% of the thickness of the cell.

## 108 RESULTS

109 An object looks like a line or rod shape with a length of 1–10  $\mu\text{m}$  was found to be  
110 trapped at the focal point when the laser beam was irradiated. Hereafter, these objects are  
111 referred as “line-shaped object”. The optical microscope images of a nanosheet colloid  
112 before and after irradiation with a linearly polarized laser beam are shown in Figure 2.  
113 Before laser irradiation, many line-shaped objects were observed within the microscope  
114 field (Figure 2a). The line-shaped objects were moved and/or appeared and disappeared  
115 owing to the focusing and de-focusing by three-dimensional Brownian motion. As  
116 described in the discussion, the line-shaped objects were attributed to be nanosheets  
117 oriented with their in-plane direction perpendicular to the cell surface. The image after 15  
118 s of continuous laser irradiation (Figure 2b) indicates no apparent change at the focal  
119 point, whereas the Brownian motion seen over the entire microscope field was  
120 continuously observed. After 30 s of continuous laser irradiation, a line-shaped object  
121 appeared near the focal point (Figure 2c). This line-shaped object was moved toward the  
122 focal point and then was completely trapped at the focal point after 34 s of continuous  
123 laser irradiation (Figure 2d) and no longer disappeared during laser irradiation. The

124 orientation of the object was parallel to the polarization direction of the incident laser  
125 beam. The time required for trapping of the line-shaped object was from 20 s to 34 s.

126 The line-shaped object was gradually released when the laser irradiation was ceased.  
127 The line-shaped object trapped at the focal point began the Brownian motion again just  
128 after the laser irradiation was ceased (Figure 3a). The object was then gradually diffused  
129 and became blurred (Figure 3b and 3c). At 15 s after the laser irradiation ceased (Figure  
130 3d), the image was essentially the same as that before laser irradiation (see Figure 2a).

131 The line-shaped object was repeatedly trapped at the focal point by on-off switching  
132 of the laser irradiation. Upon irradiation with the laser beam 15 s after the laser irradiation  
133 ceased, the line-shaped object was re-trapped at the focal point after approximately 30 s  
134 of continuous laser irradiation (Figure 4a). After the laser irradiation was ceased again,  
135 the re-trapped line-shaped object diffused and was no longer observed (Figure 4b). The  
136 re-trapping and releasing was repeated by further on-off switching cycles of the laser  
137 irradiation (Figure 4c and Figure 4d).

138 Figure 5 shows that the trapped line-shaped object was rotated following rotation of  
139 the polarization direction of the incident laser beam. A trapped nanosheet (Figure 5a) by  
140 irradiation of a laser beam with a polarization direction of  $45^\circ$  with respect to the viewing  
141 direction can be seen. When the polarization direction was rotated clockwise by  $45^\circ$ , the



142 line-shaped object was also rotated clockwise by  $45^\circ$  (Figure 5b). When the polarization  
143 direction was sequentially rotated by a further  $45^\circ$ , the line-shaped object was rotated  
144 following the rotation of the polarization direction (Figure 5c and Figure 5d). The rotation  
145 of the trapped line-shaped object followed that of the polarization direction in real-time  
146 until the upper limit of the rotation speed of the employed experimental setup, which was  
147  $0.4 \pi$  rad/s.

## 148 DISCUSSION

149 The line-shaped object observed in Figures 2, 4 and 5 was proposed to be a nanosheet  
150 oriented with the in-plane direction parallel to the propagation direction of the laser beam.  
151 When a nanosheet orients its in-plane direction parallel to the propagation direction of an  
152 incident laser beam, the nanosheet should be observed as a line. In fact, the orientation of  
153 the nanosheet was also confirmed by polarized optical microscopy observation (data not  
154 shown). The image before laser irradiation was dark. After approximately 30 s of  
155 continuous laser irradiation, which was the time when the nanosheet was trapped at the  
156 focal point, a birefringent line appeared. The birefringence was ascribed to the orientation  
157 of the nanosheet with its in-plane direction perpendicular to the cell surface (Nakato *et*  
158 *al.*, 2011).

159 The orientation behavior of a nanosheet by laser irradiation can be considered as an

160 analogy of the orientation manipulation of 1D particles. In general, a focused laser beam  
161 provides two types of forces as a radiation pressure on a particle (Ashkin, 1992; Harada  
162 and Asakura, 1996). One is a scattering force which is applied toward the propagation  
163 direction of the incident laser beam to the object. Namely, when the scattering force is  
164 applied to an object, the object moves along the propagation direction of the incident laser  
165 beam. The other is a gradient force which is applied perpendicular to the propagation  
166 direction of the incident laser beam. Owing to the gradient force, an object located within  
167 a focal plane is attracted to the focal point. It has been reported that 1D particles orient  
168 their long-axis parallel to the propagation direction of an incident laser beam to minimize  
169 the scattering force and then they are trapped by the gradient force when a focused laser  
170 beam is used to irradiate them (Tong *et al.*, 2010). In the case of a nanosheet, the aspect  
171 ratio of the lateral length to its thickness is approximately 1:1000. Therefore, the forces  
172 being applied in the direction perpendicular to the surface of the nanosheet are dominant  
173 and the force being applied in the direction parallel to the surface of the nanosheet is  
174 negligible. As is the case for 1D materials, a nanosheet was thought to be oriented with  
175 its in-plane direction parallel to the propagation direction of an incident laser beam so as  
176 to minimize the scattering force.

177 The appearance of a line-shaped object at the focal point can be explained by the

178 following mechanism. The thickness of the sample cell, 100  $\mu\text{m}$ , was approximately 250  
179 times larger than the depth of field. As described above, the nanosheets in the colloids  
180 randomly move by three-dimensional Brownian motion. A nanosheet coming into the  
181 optical path, including the defocus field, should be attracted to the focal point by a  
182 scattering and/or a gradient force and then the object will appear in the obtained  
183 microscope image. Continuous laser irradiation of approximately 30 s was required until  
184 the line-shaped object appeared in Figure 2c. The reason why such a long time was  
185 required is considered to arise from the low concentration of the nanosheet colloid used  
186 in this study. Hence, approximately 30 s was required for a nanosheet to come into the  
187 optical path. Actually, it was confirmed that the time required for trapping a line-shaped  
188 object became longer when the concentration was further diluted (data not shown).

189 The nanosheet trapped at the focal point was aligned with its edge parallel to the  
190 polarization direction of the incident laser beam as shown in Figure 5. This fact indicates  
191 that the alignment was determined by the optical electric field of the linearly polarized  
192 incident laser beam. For unidirectional alignment of a nanosheet, two external forces,  
193 which are orthogonal with each other, are required owing to the biaxial shape of  
194 nanosheets. This has been realized by an orthogonal application of the electric field and  
195 gravity (Nakato *et al.*, 2014; Nakato *et al.*, 2011). In this study, a unidirectional alignment

196 of 2D particles was realized by using one external stimuli consisting of two forces, which  
197 were the scattering force and the polarization direction of the laser beam. In addition, the  
198 induced alignment of the nanosheet was on-demand, as shown in Figure 4.

## 199 CONCLUSIONS

200 In this study, on-demand orientation manipulation of a nanosheet was conducted by  
201 irradiation with a linearly polarized laser beam. The nanosheet was trapped at the focal  
202 point to orient its in-plane direction parallel to the propagation direction of the incident  
203 laser beam. In addition, the alignment of the nanosheet trapped at the focal point was  
204 along the polarization direction and rotated following the rotation of the polarization  
205 direction of the incident laser beam. After laser irradiation was ceased, the trapped  
206 nanosheet diffused by Brownian motion and returned to be isotropic. This optical control  
207 of time, space and orientation of 2D particles was realized for the first time.

208 In order to maximize the functionality of 2D particles, a methodology that enables the  
209 local and on-demand orientation manipulation of 2D particles has needed. Optical  
210 manipulation established in this study should provide a powerful methodology for  
211 realizing required orientation of 2D particles and therefore should expand the application,  
212 such as optical switching and light modulation, using 2D particles including clay  
213 nanosheets

214

## ACKNOWLEDGMENTS

215 This work was supported by JSPS KAKENHI Grant Numbers 15J07557 (M.T.),  
216 15H03878 (T.N.), 17H05466 (Y.S.), and 15K13676 (J.K.), and by the Opto-Energy  
217 Research Center in Yamaguchi University. M.T. was supported financially by a JSPS  
218 Research Fellowship for Young Scientists. We thank Edanz Group  
219 ([www.edanzediting.com/ac](http://www.edanzediting.com/ac)) for editing a draft of this manuscript.

220

## REFERENCES

221 Ashkin, A. (1992) Forces of a single-beam gradient laser trap on a dielectric sphere in the  
222 ray optics regime. *Biophysical Journal*, **61**, 569-582.

223 Ashkin, A., Dziedzic, J. M., Bjorkholm, J. E., and Chu, S. (1986) Observation of a single-  
224 beam gradient force optical trap for dielectric particles. *Optics Letters*, **11**, 288-290.

225 Dholakia, K., Reece, P., and Gu, M. (2008) Optical micromanipulation. *Chemical Society*  
226 *Reviews*, **37**, 42-55.

227 Harada, Y. and Asakura, T. (1996) Radiation forces on a dielectric sphere in the Rayleigh  
228 scattering regime. *Optics Communications*, **124**, 529-541.

229 Lehmuskero, A., Johansson, P., Rubinsztein-Dunlop, H., Tong, L., and Käll, M. (2015)  
230 Laser trapping of colloidal metal nanoparticles. *ACS Nano*, **9**, 3453-3469.

231 Miyamoto, N. and Nakato, T. (2004) Liquid Crystalline Nanosheet Colloids with

232 Controlled Particle Size Obtained by Exfoliating Single Crystal of Layered Niobate  
233  $K_4Nb_6O_{17}$ . *The Journal of Physical Chemistry B*, **108**, 6152-6159.

234 Nakato, T., Kawamata, J., and Takagi, S. (2017) *Inorganic nanosheets and nanosheet-*  
235 *based materials*. Springer, Japan.

236 Nakato, T., Nakamura, K., Shimada, Y., Shido, Y., Houryu, T., Imura, Y., and Miyata, H.  
237 (2011) Electrooptic response of colloidal liquid crystals of inorganic oxide nanosheets  
238 prepared by exfoliation of a layered niobate. *Journal of Physical Chemistry C*, **115**, 8934-  
239 8939.

240 Nakato, T., Nono, Y., and Mouri, E. (2017) Textural diversity of hierarchical macroscopic  
241 structures of colloidal liquid crystalline nanosheets organized under electric fields.  
242 *Colloids and Surfaces A: Physicochemical and Engineering Aspects*, **522**, 373-381.

243 Nakato, T., Nono, Y., Mouri, E., and Nakata, M. (2014) Panoramic organization of  
244 anisotropic colloidal structures from photofunctional inorganic nanosheet liquid crystals.  
245 *Physical Chemistry Chemical physics*, **16**, 955-962.

246 Neves, A. A. R., Camposeo, A., Pagliara, S., Saija, R., Borghese, F., Denti, P., Iatì, M. A.,  
247 Cingolani, R., Maragò, O. M., and Pisignano, D. (2010) Rotational dynamics of optically  
248 trapped nanofibers. *Optics Express*, **18**, 822-830.

249 Ohlinger, A., Nedev, S., Lutich, A. A., and Feldmann, J. (2011) Optothermal escape of

250 plasmonically coupled silver nanoparticles from a three-dimensional optical trap. *Nano*  
251 *Letters*, **11**, 1770-1774.

252 Okada, T., Oguchi, J., Yamamoto, K., Shiono, T., Fujita, M., and Iiyama, T. (2015)  
253 Organoclays in water cause expansion that facilitates caffeine adsorption. *Langmuir*, **31**,  
254 180-187.

255 Schoonheydt, R. A. (2014) Functional hybrid clay mineral films. *Applied Clay Science*,  
256 **96**, 9-21.

257 Suzuki, Y., Tenma, Y., Nishioka, Y., and Kawamata, J. (2012) Efficient nonlinear optical  
258 properties of dyes confined in interlayer nanospaces of clay minerals. *Chemistry-An Asian*  
259 *Journal*, **7**, 1170-1179.

260 Tominaga, M., Oniki, Y., Mochida, S., Kasatani, K., Tani, S., Suzuki, Y., and Kawamata,  
261 J. (2016) Clay–organic hybrid films exhibiting reversible fluorescent color switching  
262 induced by swelling and drying of a clay mineral. *The Journal of Physical Chemistry C*,  
263 **120**, 23813-23822.

264 Tong, L., Miljković, V. D., and Käll, M. (2010) Alignment, rotation, and spinning of  
265 single plasmonic nanoparticles and nanowires using polarization dependent optical forces.  
266 *Nano Letters*, **10**, 268-273.

267 Won, J., Inaba, T., Masuhara, H., Fujiwara, H., Sasaki, K., Miyawaki, S., and Sato, S.

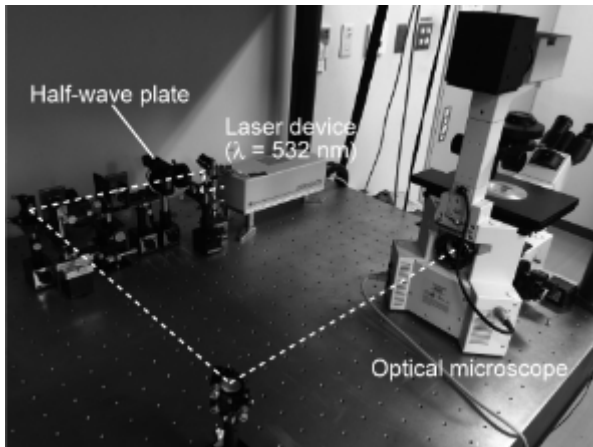
268 (1999) Photothermal fixation of laser-trapped polymer microparticles on polymer  
269 substrates. *Applied Physics Letters*, **75**, 1506-1508.

270 Wright, W. H., Sonek, G. J., and Berns, M. W. (1994) Parametric study of the forces on  
271 microspheres held by optical tweezers. *Applied Optics*, **33**, 1735-1748.

272 Wu, M., Ling, D., Ling, L., Li, W., and Li, Y. (2017) Stable optical trapping and sensitive  
273 characterization of nanostructures using standing-wave raman tweezers. *Scientific*  
274 *Reports*, **7**, 42930.

275 Yan, Z., Jureller, J. E., Sweet, J., Guffey, M. J., Pelton, M., and Scherer, N. F. (2012)  
276 Three-dimensional optical trapping and manipulation of single silver nanowires. *Nano*  
277 *Letters*, **12**, 5155-5161.



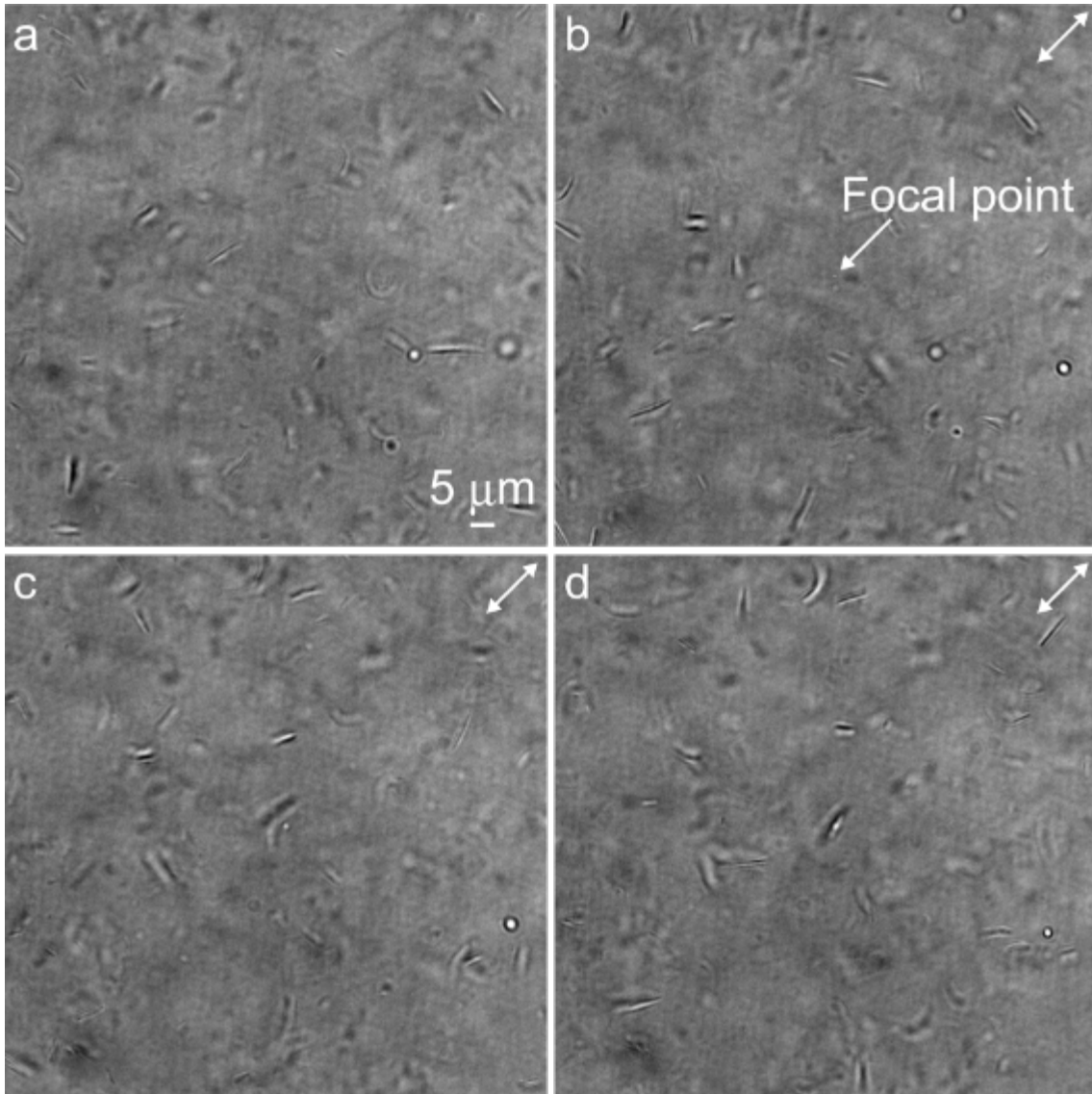


278

279 Figure 1. Photograph of the experimental setup. The broken line indicates the beam path

280 of the laser.

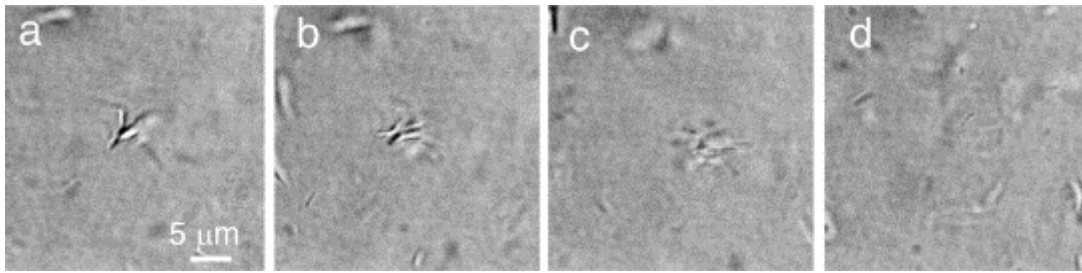
281



282

283 Figure 2. Optical microscopy images of a niobate nanosheet colloid (a) before laser  
284 irradiation and after (b) 15 s, (c) 30 s, (d) 34 s of continuous laser irradiation with a  
285 linearly polarized laser beam. The very small white point shown in (b) represents the focal  
286 spot with a diameter of 0.4 μm. The white arrow indicates the polarization direction.

287

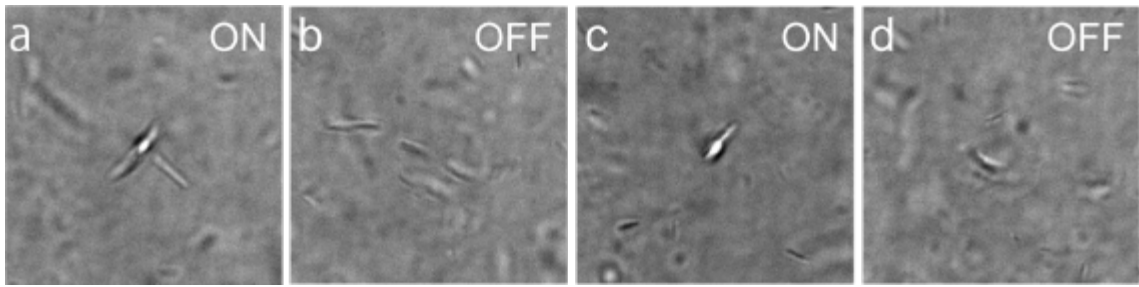


288

289 Figure 3. Optical microscopy images of a niobate nanosheet colloid (a) 0 s, (b) 2 s, (c) 10

290 s, (d) 15 s after laser irradiation ceased.

291

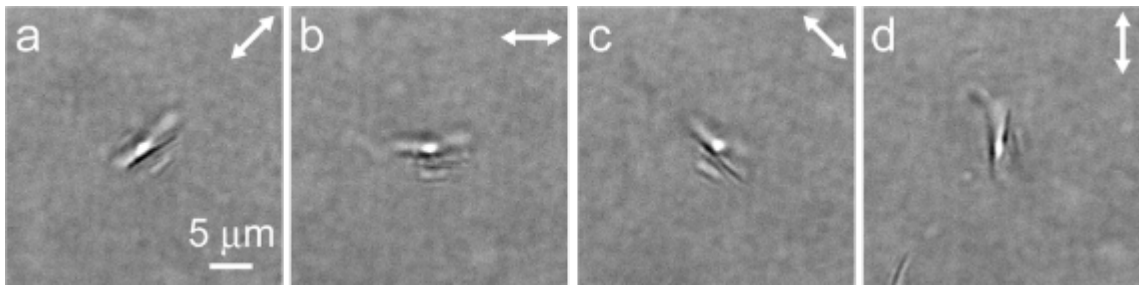


292

293 Figure 4. Optical microscopy images of re-trapped and released line-shaped objects by

294 on-off switching of the laser irradiation.

295



296

297 Figure 5. Optical microscopy images of a niobate nanosheet colloid under rotation of the

298 polarization direction of the incident laser beam. The white arrows indicate the

299 polarization direction.